

Efficient Ground-State Cooling of Large Trapped-Ion Chains with an Electromagnetically-Induced-Transparency Tripod Scheme

L. Feng^{1,*}, W. L. Tan¹, A. De¹, A. Menon¹, A. Chu¹, G. Pagano^{1,2}, and C. Monroe¹
¹*Joint Quantum Institute, Center for Quantum Information and Computer Science, and Department of Physics, University of Maryland, College Park, Maryland 20742, USA*
²*Department of Physics and Astronomy, Rice University, 6100 Main Street, Houston, Texas 77005, USA*



(Received 11 April 2020; accepted 12 June 2020; published 29 July 2020)

We report the electromagnetically-induced-transparency (EIT) cooling of a large trapped $^{171}\text{Yb}^+$ ion chain to the quantum ground state. Unlike conventional EIT cooling, we engage a four-level tripod structure and achieve fast sub-Doppler cooling over all motional modes. We observe simultaneous ground-state cooling across the complete transverse mode spectrum of up to 40 ions, occupying a bandwidth of over 3 MHz. The cooling time is observed to be less than 300 μs , independent of the number of ions. Such efficient cooling across the entire spectrum is essential for high-fidelity quantum operations using trapped ion crystals for quantum simulators or quantum computers.

DOI: [10.1103/PhysRevLett.125.053001](https://doi.org/10.1103/PhysRevLett.125.053001)

The laser cooling of mechanical oscillators to their motional ground state is an ongoing pursuit in quantum metrology, simulation, and computation [1–4]. In particular, the localization of individual atoms to well below optical wavelengths (the “Lamb-Dicke” regime) is a prerequisite for high fidelity quantum control of atomic systems [1,5]. In large trapped-ion crystals, quantum entangling gates exploit the collective motion of the ions [6,7]. This motion must be prepared near the ground state in a cooling process that competes with heating from the coupling to the environment [8,9]. It is therefore critical to develop new methods to achieve high-bandwidth and fast cooling of all the motional modes used as a quantum bus for quantum information processing.

Resolved sideband cooling (RSC) is a general tool for cooling mechanical oscillators, and for trapped ions it is the standard method for cooling to the ground state [1,10–12]. However, the RSC time typically grows linearly with the total mass of the oscillator, or the number of trapped ions in the chain. This scaling can be improved for large chains by implementing a parallel RSC strategy with single-ion addressing [13].

Electromagnetically induced transparency (EIT) cooling of trapped ions and atoms is another well-known ground-state cooling method [14–20]. It exploits quantum interference in a three-level Λ system [21] to create a tunable narrow spectroscopic feature tailored to the atomic motion for efficient cooling. Applied to trapped ions, EIT cooling allows simultaneous ground state cooling over a large portion of the motional spectrum without the need for single-ion addressing [22–24]. Extensions of EIT cooling beyond the simple three-level system have stimulated several theoretical [25–27] and experimental [28–30] studies. This extension is important for quantum

information applications with trapped-ion hyperfine qubits [7,31], whose atoms feature four or more atomic ground states. Here, we demonstrate EIT cooling with a four-level tripod structure in a chain of up to 40 $^{171}\text{Yb}^+$ ions. We achieve fast ground-state cooling of nearly all motional modes of the chain, occupying a broadband spectrum of more than 3 MHz, in a time ($<300 \mu\text{s}$) that is independent of the number of ions.

The EIT cooling of the tripod $^{171}\text{Yb}^+$ system is implemented on the $^2S_{1/2}|F=1\rangle \leftrightarrow ^2P_{1/2}|F'=0\rangle \equiv |e\rangle$ transition at an optical wavelength of 369.5 nm and having a natural linewidth of $\Gamma = 2\pi \times 19.6 \text{ MHz}$. A constant magnetic field $B_0 = 5.5 \text{ G}$ applied along the y axis [Fig. 1(a)] provides a Zeeman shift of $\pm\Delta_B/2\pi = \pm 7.7 \text{ MHz}$ for the $|\pm 1\rangle \equiv |F=1, m_F = \pm 1\rangle$ states with respect to the $|0\rangle \equiv |F=1, m_F = 0\rangle$ state [Fig. 1(b)]. The EIT laser configuration involves two beams simultaneously and globally addressing the ions, with three components of polarization, as depicted in Fig. 1(b). The beam perpendicular to the ion chain is the strong pump beam, with a large component of σ^- and a small component of σ^+ polarization, with the power ratio controlled by a birefringent wave plate. The beam along the chain of ions is the weak probe beam with π polarization.

This tripod level configuration can be reduced to an effective Λ system by setting the frequency of the σ^- (pump) and the π (probe) components near two-photon resonance. The σ^+ component is derived from the same laser as of σ^- , therefore it is naturally detuned from any two-photon resonance because of the Zeeman shift, but serves to remove population from the $|-1\rangle$ state by off-resonant scattering [Fig. 1(b)].

To understand this simplification, we consider the tripod system interacting with the EIT lasers [Fig. 1(b)], where Ω_i

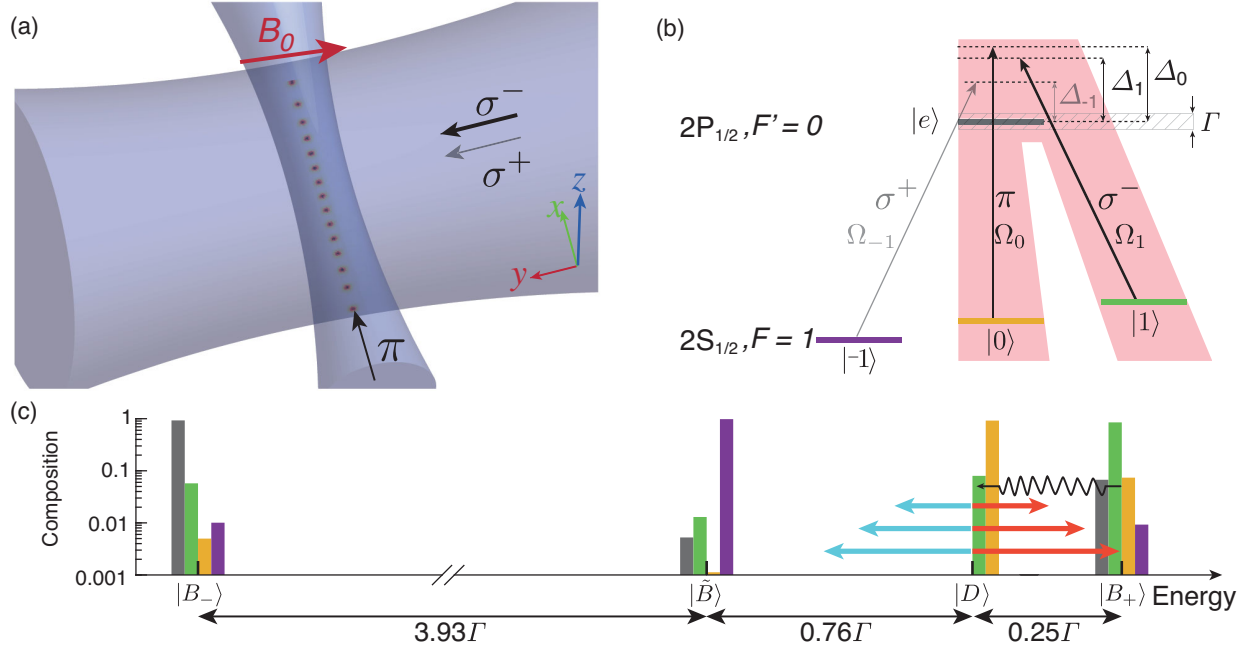


FIG. 1. (a) Configuration of the EIT cooling lasers applied to a chain of trapped ions. The σ^\pm pump beam propagates perpendicular to the chain, while the π probe beam propagates along the chain axis (x). (b) Bare atomic energy levels of the tripod $^{171}\text{Yb}^+$ structure with coupling lasers for the EIT cooling, where the pink shading illustrates the effective EIT Λ system. (c) Eigenstate compositions in the dressed-state energy levels, with the color code indicating the composition of the dressed eigenstates in terms of bare atomic states ($|0\rangle$): orange, $|1\rangle$: green, $|-1\rangle$: purple, and $|e\rangle$: gray). The blue and red arrows indicate upper and lower sideband transitions driven by motion of the ions. The black wavy arrow indicates spontaneous decay. The Rabi frequencies are $\Omega_1 = 2.0\Gamma$, $\Omega_0 = 0.35\Gamma$, and $\Omega_{-1} = 0.7\Gamma$. The detunings are set to $\Delta_0 = \Delta_1 = 4.47\Gamma$, and $\Delta_{-1} = 3.69\Gamma$.

is the Rabi frequency of the laser beam that couples the ground state $|i\rangle$ ($i = \pm 1, 0$) to the excited state $|e\rangle$ with detuning of Δ_i . We set $\Delta_0 = \Delta_1 \equiv \Delta$ and $\Delta_{-1} = \Delta - 2\Delta_B$ then obtain the eigenstates. A singular dark eigenstate $|D\rangle$ consists of the $|0\rangle$ and $|1\rangle$ atomic states while two bright eigenstates $|B_\pm\rangle$ contain a significant fraction of the excited state $|e\rangle$ along with a negligible fraction of $|-1\rangle$ [Fig. 1(b)]. The corresponding eigenvalues are $E_D \approx \Delta$ and $E_{B_\pm} \approx \frac{1}{2}(\Delta \pm \sqrt{\Delta^2 + \Omega_0^2 + \Omega_1^2})$, where we use $\hbar = 1$. The fourth remaining eigenstate $|\bar{B}\rangle$ is another bright state consisting mostly of the $|-1\rangle$ state with a tiny fraction of the excited state $|e\rangle$, and largely decoupled from the bare atomic states $|0\rangle$ and $|1\rangle$. Thus we can ignore the $|-1\rangle$ state and consider just the effective Λ system comprising $|e\rangle, |0\rangle$ and $|1\rangle$ [Fig. 1(c)] (see Supplemental Material [32]).

When the EIT beams are applied to stationary ions, the steady state population is trapped in the dark state irrespective of its initial state [21]. However, the ion motion can drive the population out of the dark state. When we set $E_{B_\pm} - E_D$ close to the oscillation frequency, the ions lose a quantum of vibrational energy as they are flipped from the dark state $|D\rangle$ to the bright state $|B_\pm\rangle$. The population in the bright state subsequently spontaneously decays back to the dark state $|D\rangle$. In the Lamb-Dicke regime, the ions recoil with very low probability [1], so this EIT absorption and emission process completes the cooling cycle, similar to RSC.

We estimate the limits of EIT cooling by considering the above cooling process balanced with heating arising from off-resonant scattering through the upper motional sidebands of the $|D\rangle \leftrightarrow |B_\pm\rangle$ transitions. We calculate the EIT absorption spectrum by using a master equation for the full tripod system (see Supplemental Material [32]), and express the EIT cooling limit as the steady-state average phonon number of a motional mode at frequency ω [1,25],

$$\bar{n}_\omega = \frac{\rho_{ee}(\Delta_0) + \rho_{ee}(\Delta_0 - \omega)}{\rho_{ee}(\Delta_0 + \omega) - \rho_{ee}(\Delta_0 - \omega)}. \quad (1)$$

Here, $\rho_{ee}(\Delta_0)$ and $\rho_{ee}(\Delta_0 \pm \omega)$ are the calculated steady-state populations of the excited state $|e\rangle$ at the carrier and sidebands. In order to apply EIT to multiple modes, the idea is to set the Rabi frequencies Ω_i and detunings Δ_i to produce a low cooling limit for a wide spectrum of modes, as shown in Fig. 2.

In this work, we employ a cryogenic trapped-ion apparatus [33] based on a linear Paul trap that confines the ions with transverse center-of-mass (COM) frequencies $(\omega_\alpha, \omega_\beta) = 2\pi \times (4.45, 4.30 \text{ MHz})$, and axial frequency $\omega_{\text{ax}} = 2\pi \times (0.29\text{--}0.39 \text{ kHz})$, depending on the number of ions. Because both principal axes of transverse motion have components along the wave vector difference between the EIT pump and probe beams [y axis in Fig. 1(a)], both directions of transverse motion are cooled by EIT.

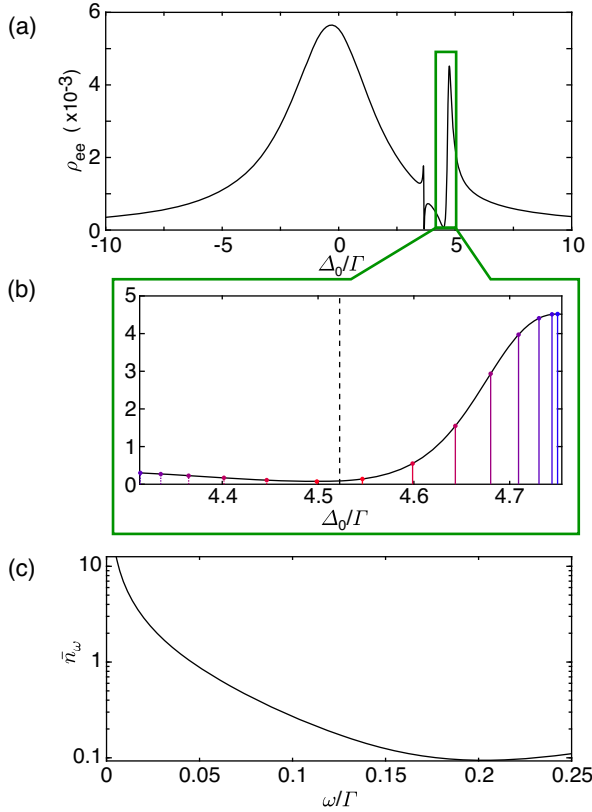


FIG. 2. (a) The Fano-like absorption profile of EIT, expressed as the excited state population ρ_{ee} as a function of probe laser detuning Δ_0 , calculated by numerically solving the steady-state solution of the master equation (see Supplemental Material [32]) with the same parameters as that in Fig. 1(c). (b) The expanded view of the EIT profile at the dark resonance of interest. The black dashed line marks the probe frequency during cooling. The red to blue lines mark several example transverse mode frequencies with their value increasing as the color continuously changing from red to blue. Dashed (solid) lines indicate upper (lower) sidebands. (c) Calculated steady-state average phonon number of motional mode with frequency ω based on EIT theory (see Supplemental Material [32]).

Following this cooling, we measure the vibrational population of the transverse modes by performing conventional sideband spectroscopy. We use a pair of counterpropagating 355 nm laser beams to drive motional-sensitive stimulated Raman transitions between qubit states $|\downarrow\rangle \equiv {}^2S_{1/2}|F=0, m_F=0\rangle$ and the $|\uparrow\rangle \equiv {}^2S_{1/2}|F=1, m_F=0\rangle$ [34], and measure the lower/upper sideband ratio R_ω for each transverse mode and extract $\bar{n}_\omega = R_\omega/(1 - R_\omega)$ [1] (see Supplemental Material [32] for details).

We first demonstrate the EIT cooling scheme for a single $^{171}\text{Yb}^+$ ion. Beside the main EIT beams generated from a 369.5 nm diode laser, a 14.7 GHz sideband is added to the pump beam to avoid population trapping in the $|\downarrow\rangle$ state [35]. The Rabi frequency and laser detuning of the EIT pump and probe beams are optimized to achieve the best cooling for the transverse mode at ω_α (Fig. 3, inset).

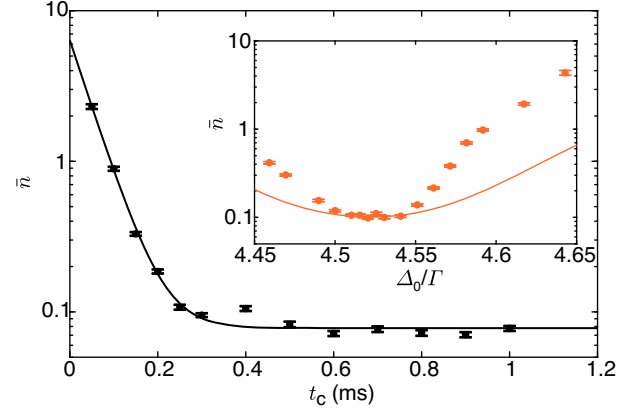


FIG. 3. Measured mean phonon number (black dots) as a function of EIT cooling duration t_C extracted from the Raman spectroscopy for one transverse mode of the motion at $\omega_\alpha = 2\pi \times 4.45$ MHz for a single ion. The solid curve is a fit of the data to an exponential decay plus an offset term. The inset shows measurements of steady-state mean phonon number with various settings of the probe detuning Δ_0 , along with the master equation theory (solid line, see Supplemental Material [32]). The Rabi frequencies in the experiment are $\Omega_1 = 2.0\Gamma$, $\Omega_0 = 0.76\Gamma$, and $\Omega_{-1} = 0.8\Gamma$. The detunings are set to $\Delta_1 = 4.5\Gamma$, $\Delta_0 = 4.54\Gamma$ and $\Delta_{-1} = 3.69\Gamma$, respectively. We see qualitative agreement between theory and experiment, and good quantitative agreement for probe detunings used in the experiment near the optimal cooling limits. The error bars indicate one standard statistical error.

The measured optimal thermal phonon number agrees with a simple theoretical treatment, but deviates when the beams are tuned away from EIT dark resonance (see Supplemental Material [32]). We measure the steady-state phonon number for various cooling times t_C and extract a $1/e$ cooling time of $48 \mu\text{s}$ and the steady-state average phonon number of $\bar{n}_\omega = 0.08$ with a cooling rate of 8.4×10^4 quanta/s (Fig. 3).

We next perform EIT cooling on chains of $N = 5, 15, 23$, and 40 trapped ions following the same experimental procedure, with results shown in Figs. 4(a)–4(d). We see a total of $2N$ sideband features corresponding to both sets of transverse modes. We apply the EIT cooling for a fixed time $t_C = 300 \mu\text{s}$, independent of the number of ions, and observe a strong suppression of the lower sidebands compared to the upper sidebands, indicating efficient cooling of the motional modes close to their ground states. We observe average phonon numbers as low as $\bar{n}_\omega = 0.04 \pm 0.01$ for particular modes, and $\bar{n}_\omega < 0.54$ for all modes over a 3 MHz bandwidth [Fig. 4(e)], using the same amount of cooling time as that for a single ion. The EIT cooling method is thus found to be independent of the number of ions or modes, assuming that the sideband spectrum of modes remains within the cooling bandwidth and there is sufficient laser power available to provide the same intensity on each ion. The cooling results agree well with the master equation theory at the optimal cooling configuration since the heating from imperfect polarization is minimized (see Supplemental Material [32]).

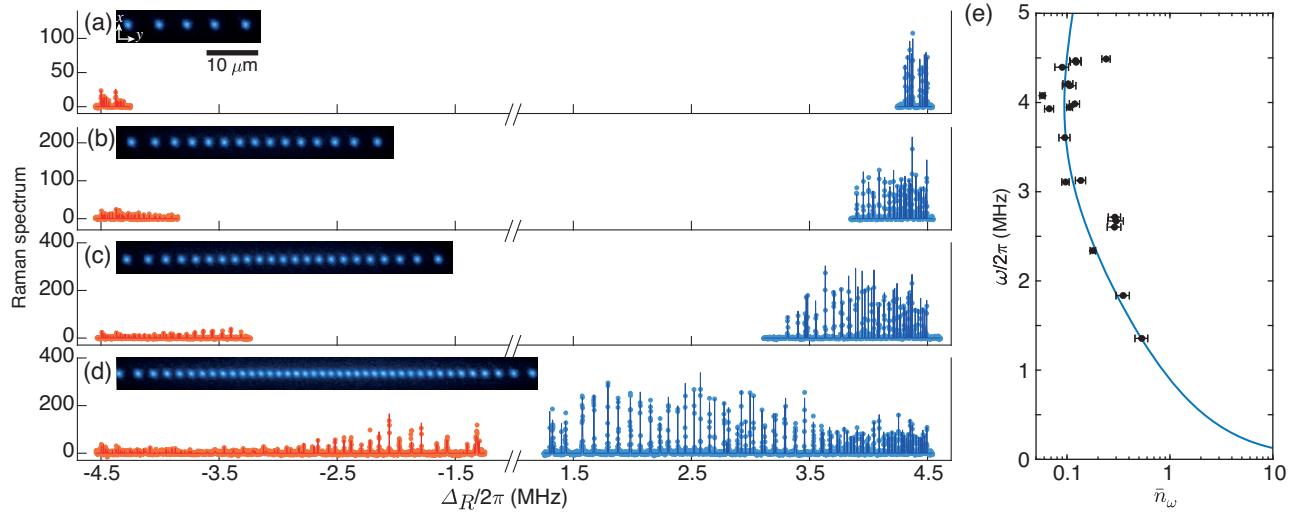


FIG. 4. The lower (red) and upper (blue) motional sideband spectrum for a chain of 5, 15, 23, and 40 ions are shown in (a), (b), (c), and (d), respectively, after EIT cooling. The horizontal axis is the Raman detuning from the qubit carrier transition. The highest frequency (COM) modes near 4.45 MHz do not change as the number of ions increases. With each additional ion, two more transverse modes appear at lower frequencies. The strong sideband asymmetry indicates ground-state cooling of the corresponding motional modes, over a large cooling bandwidth of 3 MHz. The dots indicate experiment data, solid lines are Gaussian fits to guide the eye. The inset shows the ion chain in the corresponding cooling experiment. (e) The extracted steady-state phonon number of select transverse modes across the motional band of a 40-ion chain. The dots indicate the experiment data and the solid line is the theoretical prediction. The error bars indicate one standard statistical error.

Finally, we investigate the cooling performance of a sequential combination of EIT cooling, then RSC of select modes for a chain of 36 ions (see Supplemental Material [32]). We observe that this combination provides better cooling efficiency than either method individually. In the future, EIT cooling may be optimized further in the tripod system by applying a stronger σ^+ beam further detuned from the spectator bright state $|\tilde{B}\rangle$, and should result in even larger cooling bandwidths, lower phonon populations, and shorter cooling times, as predicted by theoretical models (see Supplemental Material [32]). Overall, the EIT cooling mechanism discussed here appears to be an excellent tool for the quantum control of large chains of atomic ions for quantum information applications.

We acknowledge early discussions with Kristi Beck, Michael Foss-Feig, and Tobias Grass. This work is supported by the Multidisciplinary University Research Initiative from Army Research Office on Modular Quantum Systems, the DARPA DRINQS program, the DOE BES Award No. de-sc0019449, the DOE HEP Award No. de-sc0019380, and the Seed-Funding Program of the NSF Physics Frontier Center at Joint Quantum Institute.

*leifeng@umd.edu

- [1] D. Leibfried, R. Blatt, C. Monroe, and D. Wineland, *Rev. Mod. Phys.* **75**, 281 (2003).
 [2] A. Urvoy, Z. Vendeiro, J. Ramette, A. Adiyatullin, and V. Vuletić, *Phys. Rev. Lett.* **122**, 203202 (2019).

- [3] T. J. Kippenberg and K. J. Vahala, *Science* **321**, 1172 (2008).
 [4] H. J. Metcalf and P. van der Straten, *Laser Cooling and Trapping* (Springer-Verlag, New York, NY, 1999).
 [5] M. Saffman, *Natl. Sci. Rev.* **6**, 24 (2018).
 [6] D. Wineland and R. Blatt, *Nature (London)* **453**, 1008 (2008).
 [7] C. Monroe and J. Kim, *Science* **339**, 1164 (2013).
 [8] Q. A. Turchette, C. J. Myatt, B. E. King, C. A. Sackett, D. Kielpinski, W. M. Itano, C. Monroe, and D. J. Wineland, *Phys. Rev. A* **62**, 053807 (2000).
 [9] M. Brownnutt, M. Kumph, P. Rabl, and R. Blatt, *Rev. Mod. Phys.* **87**, 1419 (2015).
 [10] F. Diedrich, J. C. Bergquist, W. M. Itano, and D. J. Wineland, *Phys. Rev. Lett.* **62**, 403 (1989).
 [11] C. Monroe, D. M. Meekhof, B. E. King, S. R. Jefferts, W. M. Itano, D. J. Wineland, and P. Gould, *Phys. Rev. Lett.* **75**, 4011 (1995).
 [12] B. E. King, C. S. Wood, C. J. Myatt, Q. A. Turchette, D. Leibfried, W. M. Itano, C. Monroe, and D. J. Wineland, *Phys. Rev. Lett.* **81**, 1525 (1998).
 [13] J. S. Chen, K. Wright, N. C. Pienti, D. Murphy, K. M. Beck, K. Landsman, J. M. Amini, and Y. Nam, *arXiv:2002.04133*.
 [14] G. Morigi, J. Eschner, and C. H. Keitel, *Phys. Rev. Lett.* **85**, 4458 (2000).
 [15] C. F. Roos, D. Leibfried, A. Mundt, F. Schmidt-Kaler, J. Eschner, and R. Blatt, *Phys. Rev. Lett.* **85**, 5547 (2000).
 [16] K. Xia and J. Evers, *Phys. Rev. Lett.* **103**, 227203 (2009).
 [17] T. Kampschulte, W. Alt, S. Manz, M. Martinez-Dorantes, R. Reimann, S. Yoon, D. Meschede, M. Bienert, and G. Morigi, *Phys. Rev. A* **89**, 033404 (2014).

- [18] Y. Guo, K. Li, W. Nie, and Y. Li, *Phys. Rev. A* **90**, 053841 (2014).
- [19] E. Haller, J. Hudson, A. Kelly, D. A. Cotta, B. Peaudecerf, G. D. Bruce, and S. Kuhr, *Nat. Phys.* **11**, 738 (2015).
- [20] G. Morigi, *Phys. Rev. A* **67**, 033402 (2003).
- [21] B. Lounis and C. Cohen-Tannoudji, *J. Phys. II (France)* **2**, 579 (1992).
- [22] E. Jordan, K. A. Gilmore, A. Shankar, A. Safavi-Naini, J. G. Bohnet, M. J. Holland, and J. J. Bollinger, *Phys. Rev. Lett.* **122**, 053603 (2019).
- [23] A. Shankar, E. Jordan, K. A. Gilmore, A. Safavi-Naini, J. J. Bollinger, and M. J. Holland, *Phys. Rev. A* **99**, 023409 (2019).
- [24] R. Lechner, C. Maier, C. Hempel, P. Jurcevic, B. P. Lanyon, T. Monz, M. Brownnutt, R. Blatt, and C. F. Roos, *Phys. Rev. A* **93**, 053401 (2016).
- [25] I. A. Semerikov, I. V. Zalivako, A. S. Borisenko, K. Y. Khabarova, and N. N. Kolachevsky, *J. Russ. Laser Res.* **39**, 568 (2018).
- [26] Y. Lu, J.-Q. Zhang, J.-M. Cui, D.-Y. Cao, S. Zhang, Y.-F. Huang, C.-F. Li, and G.-C. Guo, *Phys. Rev. A* **92**, 023420 (2015).
- [27] J. Evers and C. H. Keitel, *Europhys. Lett.* **68**, 370 (2004).
- [28] N. Scharnhorst, J. Cerrillo, J. Kramer, I. D. Leroux, J. B. Wübbena, A. Retzker, and P. O. Schmidt, *Phys. Rev. A* **98**, 023424 (2018).
- [29] S. Ejtemaee and P. C. Haljan, *Phys. Rev. Lett.* **119**, 043001 (2017).
- [30] M. Qiao, Y. Wang, Z. Cai, B. Du, P. Wang, C. Luan, W. Chen, H.-R. Noh, and K. Kim, [arXiv:2003.10276](https://arxiv.org/abs/2003.10276).
- [31] B. Blinov, D. Leibfried, C. Monroe, and D. Wineland, *Quantum Inf. Process.* **3**, 45 (2004).
- [32] See Supplemental Material at <http://link.aps.org/supplemental/10.1103/PhysRevLett.125.053001> for theoretical and numerical calculation, and Experimental method.
- [33] G. Pagano, P. W. Hess, H. B. Kaplan, W. L. Tan, P. Richerme, P. Becker, A. Kyprianidis, J. Zhang, E. Birkelbaw, M. R. Hernandez, Y. Wu, and C. Monroe, *Quantum Sci. Technol.* **4**, 014004 (2018).
- [34] D. Hayes, D. N. Matsukevich, P. Maunz, D. Hucul, Q. Quraishi, S. Olmschenk, W. Campbell, J. Mizrahi, C. Senko, and C. Monroe, *Phys. Rev. Lett.* **104**, 140501 (2010).
- [35] S. Olmschenk, K. C. Younge, D. L. Moehring, D. N. Matsukevich, P. Maunz, and C. Monroe, *Phys. Rev. A* **76**, 052314 (2007).